



LAWRENCE
LIVERMORE
NATIONAL
LABORATORY

LLNL-TR-418835

NOx Sensor Development

L. Y. Woo, R. S. Glass

October 28, 2009

Disclaimer

This document was prepared as an account of work sponsored by an agency of the United States government. Neither the United States government nor Lawrence Livermore National Security, LLC, nor any of their employees makes any warranty, expressed or implied, or assumes any legal liability or responsibility for the accuracy, completeness, or usefulness of any information, apparatus, product, or process disclosed, or represents that its use would not infringe privately owned rights. Reference herein to any specific commercial product, process, or service by trade name, trademark, manufacturer, or otherwise does not necessarily constitute or imply its endorsement, recommendation, or favoring by the United States government or Lawrence Livermore National Security, LLC. The views and opinions of authors expressed herein do not necessarily state or reflect those of the United States government or Lawrence Livermore National Security, LLC, and shall not be used for advertising or product endorsement purposes.

This work performed under the auspices of the U.S. Department of Energy by Lawrence Livermore National Laboratory under Contract DE-AC52-07NA27344.

Agreement 8697 - NO_x Sensor Development

Leta Y. Woo and Robert S. Glass

Lawrence Livermore National Laboratory

P.O. Box 808, L-184

Livermore, CA 94551-9900

(925) 423-7140; fax: (925) (423-0153); e-mail: glass3@llnl.gov

DOE Technology Manager: Jerry L. Gibbs

(202) 586-1182; fax: (202) 586-1600; e-mail: jerry.gibbs@ee.doe.gov

Contractor: Lawrence Livermore National Laboratory, Livermore, California
Prime Contract No.: W-7405-Eng-48; LLNL-TR-418835

Objectives

- Develop an inexpensive, rapid-response, high-sensitivity and selective electrochemical sensor for oxides of nitrogen (NO_x) for compression-ignition, direct-injection (CIDI) exhaust gas monitoring
- Explore and characterize novel, effective sensing methodologies based on impedance measurements
- Explore designs and manufacturing methods that could be compatible with mass fabrication
- Collaborate with industry in order to (ultimately) transfer the technology to a supplier for commercialization

Approach

- Use an ionic (O²⁻) conducting ceramic as a solid electrolyte and metal or metal-oxide electrodes
- Correlate NO_x concentration with changes in impedance by measuring the cell response to an ac signal
- Evaluate sensing mechanisms using electrochemical techniques
- Characterize aging mechanisms and the effects on long-term performance of candidate sensor materials
- Understand and develop methodology to eliminate interferences
- Collaborate with the Ford Research Center to optimize sensor materials, operating parameters, and performance and perform dynamometer on-vehicle testing

Accomplishments

- Improved design to address mechanical stability by mounting sensor on a heated alumina substrate that is suitable for packaging into a commercial sensor housing and directly attaching to the exhaust manifold for engine dynamometer tests
- Completed long-term evaluation of more advanced prototype demonstrating over 3000 h of continuous operation and stability with thermal cycling from operating temperatures (~600°C) to room temperature
- Evaluated H₂O and O₂ cross-sensitivity, successfully demonstrating the potential for O₂ compensation using a dual-frequency method that allows the background O₂ signal to be subtracted out
- Publications/Presentations/Patents:
 - Submitted Record of Invention (ROI) and filed a provisional patent

- Presented poster at the 2008 Fall Meeting of the Materials Research Society Meeting
 - Oral presentation at the 2009 DOE Hydrogen Program and Vehicle Technologies Program Annual Merit Review and Peer Evaluation Meeting
 - Oral presentation at the 215th Electrochemical Society Meeting
 - Manuscript submitted to the Journal of the Electrochemical Society

Future Directions

- Develop more advanced prototypes using processes suitable for cost-effective, mass manufacturing
- Evaluate performance of prototypes, including long-term stability and cross-sensitivity, in laboratory, dynamometer, and on-vehicle tests
- Initiate the technology transfer process to a commercial entity

Introduction

NO_x compounds, specifically NO and NO₂, are pollutants and potent greenhouse gases. Compact and inexpensive NO_x sensors are necessary in the next generation of diesel (CIDI) automobiles to meet government emission requirements and enable the more rapid introduction of more efficient, higher fuel economy CIDI vehicles.¹⁻³

Because the need for a NO_x sensor is fairly recent and the performance requirements are extremely challenging, most are still in the development phase.⁴⁻⁶ Currently, there is only one type of NO_x sensor that is sold commercially, and it seems unlikely to meet more stringent future emission requirements.

Automotive exhaust sensor development has focused on solid-state electrochemical technology, which has proven to be robust for in-situ operation in harsh, high-temperature environments (e.g., the oxygen stoichiometric sensor). Solid-state sensors typically rely on yttria-stabilized zirconia (YSZ) as the oxygen-ion conducting electrolyte and then target different types of metal or metal-oxide electrodes to optimize the response.²⁻⁶

Electrochemical sensors can be operated in different modes, including amperometric (a current is measured) and potentiometric (a voltage is measured), both of which employ direct current (dc) measurements. Amperometric operation is costly due to the electronics necessary to measure the small sensor signal (nanoampere current at ppm NO_x levels), and cannot be easily improved to meet the future technical performance requirements. Potentiometric operation has not demonstrated enough promise in meeting long-term stability requirements, where the

voltage signal drift is thought to be due to aging effects associated with electrically driven changes, both morphological and compositional, in the sensor.⁷

Our approach involves impedancemetric operation, which uses alternating current (ac) measurements at a specified frequency. We have described this approach in last year's report and in several publications (See Ref. 8-10). Impedancemetric operation has shown the potential to overcome the drawbacks of other approaches, including higher sensitivity towards NO_x, better long-term stability, potential for subtracting out background interferences, total NO_x measurement, and lower cost materials and operation.⁸⁻¹⁰

Past LLNL research and development efforts have focused on characterizing different sensor materials and understanding complex sensing mechanisms.⁸⁻¹⁰ Continued effort has led to improved prototypes with better performance, including increased sensitivity (to less than 5 ppm) and long-term stability, with more appropriate designs for mass fabrication, including incorporation of an alumina substrate with an imbedded heater.

Remaining challenges include mechanical stability and sensor accuracy, which depends on cross-sensitivity to interfering gases and temperature dependency. Our most recent efforts have focused on improving two of the more advanced prototypes by addressing mechanical stability and materials processing limitations while evaluating potential tradeoffs in sensor performance and accuracy.

The ultimate goal is the transfer of this technology to a supplier for commercialization. Due to the recent economic downturn, suppliers are demanding

more comprehensive data and increased performance analysis before committing their resources to take the technology to market. Therefore, our NO_x sensor work requires a level of technology development more thorough and extensive than ever before.

Background

For an electrochemical cell with two electrodes, impedancemetric sensing requires that at least one of the electrodes act as the “sensing” electrode. The sensing electrode will have a preferable response to NO_x over other gas phase components. However, in impedancemetric sensing, both electrodes can nevertheless have an appreciable response. This contrasts to the case in potentiometric sensing where differential measurements are much more important. Therefore, the sensor design is flexible and can either contain one sensing electrode and one counter (i.e., non-sensing) electrode, or two sensing electrodes. It opens up the opportunity to use a greater variety of materials.

Previous work at LLNL focused on the role of electrode composition and microstructure and provided criteria for higher sensitivity electrodes, which depended on limiting the oxygen reaction on the electrode so that the NO_x reaction could be resolved.⁹⁻¹⁰ Our previous work suggested that impedancemetric sensing was possible with a variety of electrode materials, both metal and metal oxides, that meet general sensor criteria, which include a dense microstructure and appropriate composition to limit the catalytic activity towards oxygen.¹⁰

In more recent work, the impedancemetric sensing behavior of two compositions, gold and strontium-doped lanthanum manganite (LSM), were compared using asymmetric cell designs. LSM is an electronically conducting metal oxide. While similar overall NO_x sensitivity was observed for the two different materials and designs, differences in NO and NO_2 selectivity were noted due to influence of specific cell design characteristics on surface reactions.

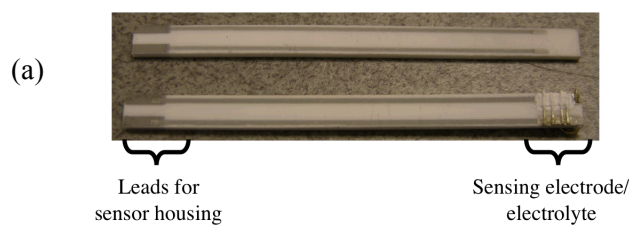
Gold sensing electrodes have demonstrated stable electrochemical performance for over 500 h of operation, the potential for low water cross-sensitivity, and a convenient wire geometry that allows the inclusion of a heated substrate. However, drawbacks of gold wire electrodes include poor mechanical performance, where the thermal mismatch with the YSZ electrolyte leads to wire delamination, and poor processing flexibility, where the melting

temperature of gold requires separate low-temperature processing steps.

Another potential drawback of gold sensing electrodes is its poor performance at higher frequencies (~ 1 kHz), which is used in the dual-frequency measurement strategy to mitigate oxygen cross-sensitivity and increase accuracy. In previous LLNL work, we demonstrated the possibility for using a separate high-frequency signal (~ 1 kHz) that is selective for oxygen (i.e., not sensitive to NO_x) in addition to the low-frequency signal (~ 5 -10 Hz), which is sensitive to both NO_x and oxygen. The oxygen contribution can then be conveniently subtracted out.⁸

Compared to gold, LSM sensing electrodes have demonstrated the potential for better performance at higher frequencies for oxygen compensation and better processing flexibility and mechanical stability due to higher melting temperatures and better thermal expansion match with the YSZ electrolyte. However, drawbacks of LSM electrodes include potential water cross-sensitivity, including water-induced drift/aging, and pose more difficult geometric considerations for incorporating a heated substrate.

Our current work focuses on addressing the drawbacks of both materials and developing more advanced prototypes that incorporate alumina substrates with imbedded heaters. The top of Fig. 1a shows the alumina substrate with an imbedded heater, which is provided by our collaborators at Ford Motor Company. The sensing electrode/electrolyte/counter electrode (i.e., cell) is located at one end of the substrate, as shown in the bottom of Fig. 1a. Leads are located on the opposite end of the substrate. This design is appropriate for packaging into a commercial sensor housing (provided by a U.S. supplier) with protective cap, as shown in Fig. 1b. The packaged sensor can then be mounted directly into the exhaust manifold during engine dynamometer testing.



(b)



Figure 1. Picture of (a) alumina substrate with imbedded heater provided by Ford Motor Company without (top) and with (bottom) sensing electrode/electrolyte/counter electrode that is suitable for packaging into a (b) commercial sensor housing.

Experimental

Two different sensing materials, Au and LSM, were investigated. Figure 2 shows a schematic of a prototype using Au wire as the sensing electrode and alumina with an imbedded Pt resistive heater as the substrate ($70 \text{ mm} \times 4 \text{ mm} \times 1 \text{ mm}$, see Fig. 1a). The substrate has a total of four leads, two leads for the Pt resistive heater located on one side, and two leads for the sensor located on the opposite side.

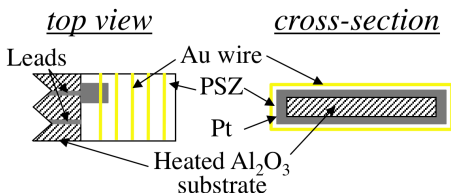


Figure 2. Schematic of more advanced NO_x prototype sensors using Au wire as the sensing electrode.

The end of the substrate was coated with Pt paste on the top, bottom, and side surfaces and fired at 1200°C . One of the substrate leads contacted the Pt counter electrode. Yttria partially-stabilized zirconia (PSZ, 3 mol% yttria doping) slurry was then applied on top of the fired Pt. Au wire was tightly wrapped around the prototype and additional PSZ slurry was applied on top of the wires and the assembly fired at 1000°C to produce the porous PSZ electrolyte. The second substrate lead for the sensor housing contacted the Au wire.

Figure 3 shows a schematic of the prototype using a dense ceramic oxide as the sensing electrode. LSM was used as the electronically conducting oxide sensing electrode. A dense pellet was prepared with commercial $(\text{La}_{0.85}\text{Sr}_{0.15})_{0.98}\text{Mn}$ oxide powder (Praxair) by pressing in a uniaxial die and sintering at 1250°C . Two pieces of LSM ($6 \text{ mm} \times 2 \text{ mm} \times 1 \text{ mm}$) were machined and attached to the top of the substrate using Pt paste and fired to 1200°C . Yttria

fully-stabilized zirconia (FSZ, 8 mol% yttria doping) slurry was applied on top of the dense LSM pieces and the assembly fired at 1000°C .

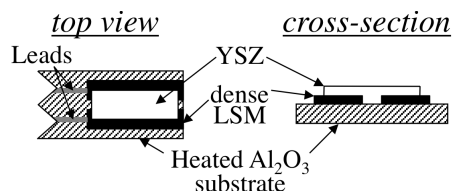


Figure 3. Schematic of more advanced NO_x prototype sensors using dense LSM as the sensing electrode.

Laboratory gas sensing experiments of sensors on heated alumina substrates were performed in a quartz tube with both electrodes exposed to the same environment. A specialized attachment (provided by Ford Motor Company) was used to make contact with the sensor and heater leads. Based on previous testing protocols and the role of the differing catalytic activity of Au and LSM in NO_x sensitivity, the prototypes with the Au wire sensors were maintained at a higher temperature (the heating element operated at a higher voltage) than the LSM sensors, 10.5 and 8.5 V, respectively.

The exact temperature corresponding to the heater voltage was not known, but was correlated with the behavior of similar prototypes that underwent furnace testing. Future prototypes may incorporate resistive temperature detectors to more accurately determine temperature. Nevertheless, Au wire and LSM sensors were previously tested at 650°C and 575°C , respectively, with similar type behavior seen in the sensors operated at 10.5 and 8.5 V, respectively.

A more detailed study of the LSM sensor and water cross-sensitivity was performed using electrodes attached to a square alumina substrate ($10 \text{ mm} \times 10 \text{ mm} \times 0.5 \text{ mm}$) without imbedded heaters. The alternative sensor geometry was more suitable for controlled temperature testing in a tube furnace. The sensor geometry was similar to that shown in Fig. 3.

Gas composition was controlled in laboratory testing by mixing air, N_2 , and a 1000 ppm NO/NO_2 feed using a standard gas handling system equipped with thermal mass flow controllers. Electrochemical measurements were performed using a Solartron 1260 Impedance Analyzer with a Solartron 1287 Electrochemical Interface.

Results and Discussion

Sensing behavior using the Au wire prototype –

Previous designs for the Au wire sensor lacked the necessary mechanical robustness for mounting into the sensor housing and attaching directly to the exhaust manifold for engine dynamometer testing. Au wire delamination was responsible for the mechanical degradation.

Previous designs used a 2D geometry and Au wire electrodes were located on only the top surface of the heated substrate. To improve adhesion of the Au wires, an improved design used a 3D geometry utilizing the top, bottom, and side surfaces of the substrate and Au wire electrodes wrapped around the entire substrate.

Previous designs also used yttria fully-stabilized zirconia (FSZ, 8 mol% yttria doping) as the electrolyte material, which has a thermal expansion coefficient of $\sim 10.5 \times 10^{-6} \text{ K}^{-1}$. The thermal mismatch between the FSZ electrolyte and Au wire electrode ($\sim 14 \times 10^{-6} \text{ K}^{-1}$) likely contributes to the mechanical degradation. To improve the thermal match, yttria partially-stabilized zirconia (PSZ, 3 mol% yttria doping) was used instead, which has an increased thermal expansion coefficient ($\sim 11 \times 10^{-6} \text{ K}^{-1}$) compared to FSZ and better matches the thermal expansion of the Au wire electrode. In addition to the increase in thermal expansion coefficient, PSZ exhibits higher toughness and lower ionic conductivity than FSZ.

Figure 4 shows the impedancemetric sensing behavior for the improved Au wire prototype in laboratory testing. The sensing signal is the phase angle response of the cell to a 100 mV ac signal at 5 Hz. In Fig. 4a, the background oxygen concentration was changed from 2 to 18.9%, as indicated at the top of the graph, and the NO concentration was changed at each oxygen level: 100, 50, 20, 10, and 0 ppm. For all changes in gas concentration, the sensor responds quickly and recovers quickly to the original baseline value ($< 10 \text{ s}$).

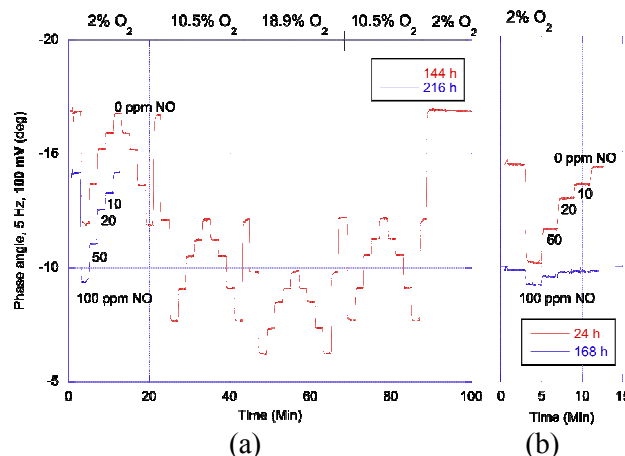


Figure 4. Sensing behavior of Au wire sensor with changes in oxygen and NO concentration at (a) 144 and 216 h of testing and (b) after a single cycle from the operating temperature to room temperature and testing at 24 and 168 h. The sensing signal shown is the phase angle response of the cell to a 100 mV ac signal at 5 Hz.

In Fig. 4a, the upper red curve shows the sensing behavior after continuous testing for 144 h using a heater voltage of 10.5 V. The lower blue curve shows the initial data (from 0 to 12 min) collected at 216 h for 2% oxygen. Only the initial data is shown at 216 h because a more compact testing protocol was used for these data and displaying the full data set would detract from figure clarity. However, similar behavior was noted for the other concentrations of oxygen at 216 h as that observed at 2% oxygen. The main point to the figure is that there was a baseline shift in going from the data set at 144 h and 216 h. The baseline shift may indicate an initial “aging” effect, which is common for electrochemical sensors. At all oxygen levels, the NO sensitivity was relatively unaffected in going from 144 to 216 h of continuous testing.

Despite the efforts to improve mechanical robustness by incorporating a 3D design strategy to improve Au wire adhesion and changing the electrolyte material for better thermal expansion matching, the performance of this sensor also degraded after thermal cycling. After the initial continuous testing of the sensor to 216 h (as shown in Fig. 4a), the sensor temperature was subsequently decreased to room temperature before returning to the testing temperature using a heater voltage of 10.5 V.

In Fig. 4b, after this single thermal cycle and holding at the operating temperature for 24 h, the upper red trace shows both a shift in the baseline and a decrease in NO sensitivity compared to the data

shown in Fig. 4a. After testing at 24 h, the sensor continued to be held at the operating temperature. At 168 h, the lower blue trace in Fig. 4b shows that the baseline continued to drift and the NO sensitivity was significantly reduced with the sensor no longer able to resolve NO concentrations less than 20 ppm. This degradation in the sensor signal indicated the need for improved materials and/or designs. As discussed in the following, the LSM prototype showed significantly better performance.

Mitigating O_2 cross-sensitivity using the Au wire and LSM prototypes – As mentioned above, we are employing a dual-frequency approach to compensate for oxygen cross-sensitivity and improve sensor accuracy.⁸

The gas flow profile for oxygen and NO compositions that was used to evaluate the phase angle response to a 100 mV ac signal at 1 kHz is shown in Fig. 5a. The high-frequency behavior (1 kHz) of the Au wire prototype is shown in Fig. 5b. The upper blue trace shows the response when only the oxygen is changing. The lower red trace shows the response when both oxygen and NO composition change. This demonstrates sensitivity towards oxygen with relatively small response to changes in NO at this frequency. However, both a considerable shift in the baseline (note beginning and end response at 2% O_2) and drift in the signal were noted. Furthermore, the amount of drift seems to increase during the course of testing. The unstable high-frequency signal with the Au wire prototype shows that this design is not suitable for compensating for oxygen cross-sensitivity.

Fig. 5c shows the high-frequency response of the LSM prototype. In contrast to the behavior noted for the Au wire prototype, the sensor responds identically to either changing both oxygen and NO (red trace) or when only changing the oxygen composition (blue trace). Furthermore, the response of the LSM prototype is much more stable and reproducible. Therefore, this prototype appears to be much more suitable for potentially mitigating oxygen cross-sensitivity and improving sensor accuracy.

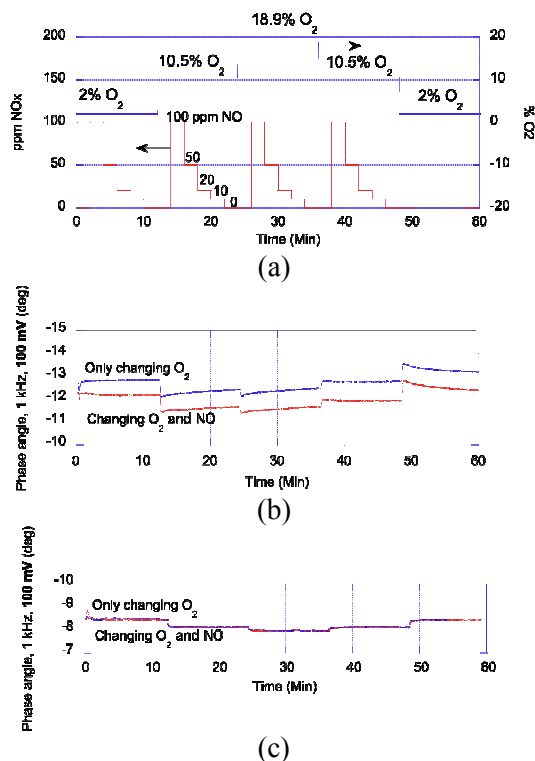


Figure 5. (a) Gas flow profile of oxygen and NO composition used for evaluating phase angle response to a 100 mV ac signal at 1 kHz. (b) Au wire prototype shows unstable signal while (c) LSM prototype shows much more stable signal suitable for potentially mitigating oxygen cross-sensitivity.

Sensing behavior using the LSM prototype –

Previous designs for the LSM sensor utilized a dense sintered LSM pellet that was then dip coated with YSZ slurry. A second counter electrode (either metal or metal oxide) was typically applied as a porous slurry and the assembly was then fired at 1000°C. Unlike the Au wire prototype, the LSM sensing electrode can not be fabricated as wires and easily attached to alumina substrates. Furthermore, in the Au wire design, the porous Pt counter electrode is processed at a higher temperature than the YSZ slurry (1200°C vs. 1000°C), which is thought to stabilize the Pt microstructure and minimize drift. However, due to the constraints of the LSM pellet design, the porous counter electrode was fired at the same temperature as the YSZ slurry (1000°C), leading to a less stable microstructure and additional aging.

To improve the LSM sensor design, pieces of LSM were machined that could then be directly attached to the alumina substrate. Furthermore, by directly attaching the LSM electrode, a symmetric

electrode design was possible (both sensing and counter electrodes were LSM) that eliminated instabilities associated with the previous porous Pt counter electrode.

Figure 6 shows the impedancemetric sensing behavior for the improved LSM prototype in laboratory testing. The sensing signal is the phase angle response of the cell to a 100 mV ac signal at 5 Hz. Similar to the experimental protocol used previously for the Au wire prototype (see Fig. 6a), the background oxygen concentration was changed from 2 to 18.9%, and the NO concentration was changed at each oxygen level: 100, 50, 20, 10, and 0 ppm. For all changes in gas concentration, the sensor responds quickly and recovers quickly to the original baseline value (< 10 s).

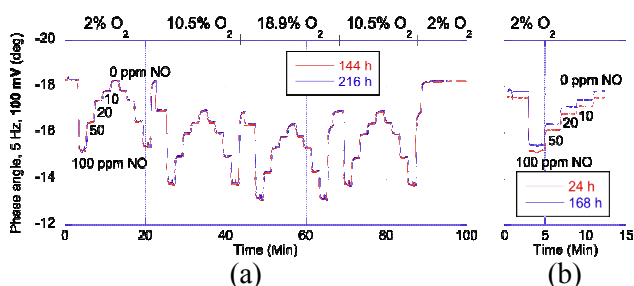


Figure 6. Sensing behavior of LSM prototype with changes in oxygen and NO concentration at (a) 144 and 216 h of testing and (b) after two cycles from the operating temperature to room temperature and testing at 24 and 168 h. The sensing signal shown is the phase angle response of the cell to a 100 mV ac signal at 5 Hz.

In Fig. 6a, there was no noticeable shift in the baseline signal after continuous testing at 144 and 216 h indicating stable sensor performance. The sensor was initially tested continuously up to 408 h (data at 144 and 216 h shown in Fig. 6a) using a heater voltage of 8.5 V. At this point, the sensor temperature was reduced to room temperature before returning to the operation temperature for another 216 h of continuous testing, at which point the sensor temperature was again cycled.

In Fig. 6b, after the two thermal cycles and holding at the operating temperature for 24 h, the lower red curve shows both a shift in the baseline and a decrease in NO sensitivity. After testing at 24 h, the sensor continued to be held at the operating temperature. At 168 h additional NO sensing data were obtained. At this point, the upper blue curve in Fig. 6b shows a slight increase in the baseline, but the NO sensitivity remained relatively unchanged, again in-

dicating better sensor stability than the previous Au wire prototype.

To evaluate long-term stability, the sensor performance of the LSM prototype, after the two thermal cycles discussed above, was monitored after testing in various water, oxygen, and NO_x concentrations. Figure 7 shows the sensing behavior of the LSM prototype with changes in oxygen and NO levels at a fixed water concentration of ~1.2% after 3120 h of total varied environment testing. All NO concentrations from 100 to 10 ppm are still clearly resolved at all oxygen levels from 2 to 18.9%. Future work includes compiling the performance data obtained over the lifetime of the sensor at various water, oxygen, and NO_x levels and improving the design and materials to enhance further the temperature control and sensor stability.

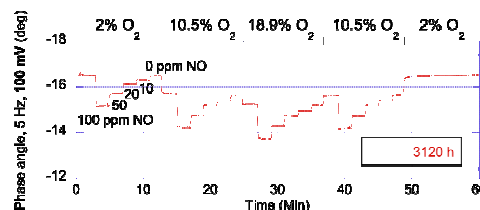


Figure 7. Sensing behavior of LSM prototype with changes in oxygen and NO levels in ~1.2% H₂O after 3120 h of continuous testing at various water, oxygen, and NO levels. The sensing signal shown is the phase angle response of the cell to a 100 mV ac signal at 5 Hz.

A more detailed study of the water cross-sensitivity of the LSM sensor was performed using a square alumina substrate (10 mm × 10 mm × 0.5 mm) without imbedded heaters onto which the LSM electrodes and FSZ electrolyte had been fabricated. The alternative sensor design was more suitable for controlled temperature testing in a tube furnace (525°C). The sensor geometry was similar to that shown in Fig. 3.

The square LSM sensor was initially tested continuously to 192 h, then thermal cycled to room temperature before returning to the operation temperature, tested continuously for another 216 h, and then thermal cycled again. In Fig. 8a, after the two thermal cycles and holding at the operating temperature (525°C) for 72 h, the lower red trace shows the sensing behavior. After testing at 72 h, the sensor continued to be held at the operating temperature. At 168 h, the upper blue trace in Fig. 8b shows almost no change in response indicating good sensor stability.

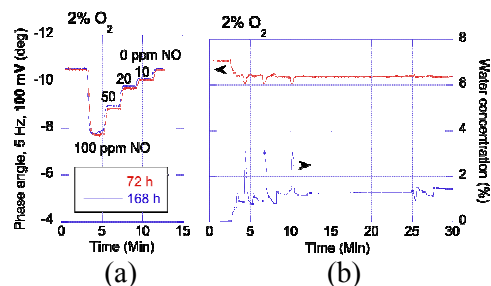


Figure 8. Sensing behavior of LSM prototype on non-heated alumina substrate at 525°C in 2% O₂ (a) with changes in NO concentration after testing for 262 h and two cycles from the operating temperature to room temperature and then additional testing at 72 and 168 h and (b) sensor response (upper red trace, values on left axis of Figure 7a) with changes in water concentration (lower blue trace, values on right axis). The sensing signal shown is the phase angle response of the cell to a 100 mV ac signal at 5 Hz.

Figure 8b shows how the sensor signal changes with water concentration. In Fig. 8b, the lower blue trace shows changes in water concentration with time (values given on the right y-axis) and the corresponding sensor signal given by the upper red trace (values given on the left y-axis in Fig. 7a). Increases in water concentration have a similar directional response in the phase angle as increases in oxygen and NO concentration.

Previous work on Au wire prototypes found that optimizing temperature significantly decreased water cross-sensitivity. Future work includes a detailed analysis of water cross-sensitivity for the LSM prototype at different temperatures.

Conclusions

Work in FY2009 has focused on more advanced NO_x sensor prototypes that incorporate an alumina substrate with an imbedded heater and modifications for improving mechanical stability. Mechanical stability is crucial for packaging into a commercial sensor housing and direct testing in the exhaust manifold. The current work builds on previous work directed at understanding sensing mechanisms and the role of material composition/microstructure. From this understanding we developed criteria that has been used to guide continuous improvements in sensor performance and design, including sensor platforms more suitable for mass manufacturing.

Although previous work demonstrated an operating NO_x prototype packaged in a sensor housing,

subsequent testing revealed insufficient long-term stability due to mechanical failure, in particular due to wire delamination in gold-based sensor prototypes. We attempted to improve the mechanical stability of the gold wire prototype by increasing the wire adhesion through geometry modification and improving the thermal expansion match between the gold electrode and zirconia electrolyte. Despite the improvements, the sensor still exhibited poor mechanical performance, especially after cycling from the high operating temperature to room temperature.

An advance to the Au wire sensor has been made by moving to LSM metal-oxide based electrodes directly attached to the alumina substrate. In addition to excellent stability and sufficient tolerance towards temperature cycling, the LSM prototype also exhibited stable high-frequency (1 kHz) oxygen selectivity, and this permits compensating for oxygen cross-sensitivity and improving sensor accuracy. Furthermore, the LSM prototype has undergone continuous testing in a variety of oxygen, water, and NO_x conditions for 3120 h and still showed good NO_x sensitivity.

References

1. N. Yamazoe, *Sens. Actuators, B*, **108**, 2 (2005).
2. R. Moos, *Int. J. Appl. Ceram. Technol.*, **2**, 401 (2005).
3. S. Akbar, P. Dutta, and C. Lee, *Int. J. Appl. Ceram. Technol.*, **3**, 302 (2006).
4. F. Menil, V. Coillard, and C. Lucat, *Sensors and Actuators B*, **67**, 1 (2000).
5. S. Zhuikov and N. Miura, *Sens. Actuators, B*, **121**, 639 (2007).
6. J. W. Fergus, *Sens. Actuators, B*, **121**, 652 (2007).
7. S. -W. Song, L. P. Martin, R. S. Glass, E. P. Murray, J. H. Visser, R. E. Soltis, R. F. Novak, and D. J. Kubinski, *J. Electrochem. Soc.*, **153**, H171 (2006).
8. L. P. Martin, L. Y. Woo, and R. S. Glass, *J. Electrochem. Soc.*, **154**, J97 (2007).
9. L. Y. Woo, L. P. Martin, R. S. Glass, and R. J. Gorte, *J. Electrochem. Soc.*, **154**, J129 (2007).
10. L. Y. Woo, L. P. Martin, R. S. Glass, W. Wang, S. Jung, R. J. Gorte, E. P. Murray, R. F. Novak, and J. H. Visser, *J. Electrochem. Soc.*, **155**, J32 (2008).

Publications/Presentations

Record of invention (IL-2048) entitled “Frequency Technique for Operating Electrochemical Sensors” submitted to the Department of Energy, November 2008. Provisional Patent Application (IL-12048, S114,480 Provisional) filed on December 18, 2008.

Poster presentation entitled “Sensing Behavior in Diesel Exhaust of Impedancemetric NO_x Gas Sensor Based on Porous YSZ/Dense Electrode Interface” at the 2008 Fall Meeting of the Materials Research, Dec. 1-5, 2008, in Boston, MA.

Oral project presentation at the 2009 DOE Hydrogen Program and Vehicle Technologies Program Annual Merit Review and Peer Evaluation Meeting, May 18-22, 2009 in Washington, D.C.

Oral presentation entitled “Impedancemetric NO_x Sensing Based On Porous Yttria-Stabilized Zirconia (YSZ) Electrolyte: Effect of Electrode Materials on Total-NO_x Sensing and Stability” at the 215th Electrochemical Society Meeting, May 25-29, 2009.

Manuscript entitled “Effect of Electrode Material and Design on Sensitivity and Selectivity for High Temperature Impedancemetric NO_x Sensors” submitted to the Journal of the Electrochemical Society, Sept. 2009.